Geophysical Research Letters

Supporting Information for

Ridge subduction sparked reorganization of the Pacific plate-mantle system 60-50 million years ago

Maria Seton[1], Nicolas Flament[1], Joanne Whittaker[2], R. Dietmar Müller[1], Michael Gurnis[3], Dan J. Bower[3]

1 EarthByte Group, School of Geosciences, University of Sydney NSW 2006, Australia

2 Institute for Marine and Antarctic Studies, University of Tasmania TAS 7001, Australia

3 Seismological Laboratory, California Institute of Technology, Pasadena, CA, USA

Contents of this file

Introduction

This file contains additional text that provides further information on the plate tectonic reconstructions and geological constraints. Four additional figures in support of the main text are also provided. The data for making these figures are either plate reconstructions, alternative seismic tomography models or numerical simulation results.

Text S1.

Plate tectonic context

The western Pacific records the birth of the Pacific plate from three "parent" plates: the Farallon, Izanagi and Phoenix 190 Ma [*Seton et al.*, 2012] (Fig. 1 and 2). Today, in the northwestern Pacific, the Japanese lineation set represents the last preserved fragment of Jurassic-Cretaceous seafloor spreading between the Pacific and Izanagi plates (Fig. 1). Seafloor spreading was continuous from at least Chron M33 until the beginning of the Cretaceous Normal Superchron (CNS) with a 24° change in spreading direction at M21, coincident with the eruption of the Shatsky Rise at the Pacific-Izanagi-Farallon triple junction [*Sager et al.*, 1999]. The youngest identified Japanese lineation (M0) displays a similar NE-SW trend to the post-M20 lineations. In our reconstruction, we follow the idea that there is no major change in spreading rate, direction or accretion between the Pacific and Izanagi plates from M0 (last dated anomaly, 120.4 Ma) (Fig. 1) to the cessation of spreading, as there is no measured change in spreading direction recorded in the fracture zones in the northwest Pacific after this time [*Matthews et al.*, 2011].

Geological evidence for ridge subduction along east Asia

Onshore geological evidence for the presence of a slab window adjacent the NW Pacific is found in the NE-SW trending Shimanto Belt in SW Japan. K-Ar dating reveals that this belt formed during two major phases, one in the late Cretaceous and one in the late Eocene-Early Oligocene, with a gap in accretion from ~55 Ma to 43 Ma [*Raimbourg et al.*, 2014]. A recent detailed structural interpretation of the Shimanto Belt [*Raimbourg et al.*, 2014] documented two main stages of extension: one in the early-mid Eocene and another in the Miocene. The early-mid Eocene extension and erosion along the margin, together with other geological considerations, such as an Eocene (46-50 Ma) metamorphic stage [*Hidetoshi Hara and Kimura*, 2008; *MacKenzie et al.*, 1992] and a change in the direction of convergence on Kyushu [*Raimbourg et al.*, 2014] and Shikoku [*Byrne and DiTullio*, 1992; *Lewis and Byrne*, 2001], suggest that a margin-wide slab detachment event is most

consistent with the available data. Additionally, combined results from cleavage and cooling ages indicates that accretion of the Okitsu melange occurred in the Cretaceous ceasing after accretion of the Nakamura Formation at ~56-55 Ma until ~43 Ma [*Raimbourg et al.*, 2014]. It is thought that the emplacement of the Okitsu Melange at ~55 Ma [*Raimbourg et al.*, 2014] required an elevated geothermal gradient [*Obayashi et al.*, 2013]. The Paleogene portion of the Shimanto Belt, the Murotohanto sub-belt, also records elevated temperatures (ranging from 225-315°) [*Hidetoshi Hara and Kimura*, 2008] and dominant seaward-verging structures [*Byrne and DiTullio*, 1992; *MacKenzie et al.*, 1992].

These elevated minimum geothermal temperatures are supportive of, but do not necessitate the presence of, an underlying slab window [*Hidetoshi Hara and Kimura*, 2008; *Lewis and Byrne*, 2001]. A possible alternative is the subduction of young oceanic crust, rather than an active mid-ocean ridge, such as the presently occurring elevated geothermal gradients along northern and southern Cascadia due to subduction of the young Juan de Fuca plate. However, alternative models for the northwest Pacific that do not invoke sub-parallel mid-ocean ridge subduction result in old, rather than young, ocean crust adjacent to the east Asian margin during the early Paleocene.

Increased palaeogeothermal gradients have also been calculated coincident with the peak heating time [*Lewis and Byrne*, 2001] and the cessation of emplacement of NE trending granite batholiths in South Korea [*Sagong et al.*, 2005] and southwestern Japan [*Nakajima*, 1996]. It may be tempting to link this cessation of granite batholith emplacement to the initiation of the Izu-Bonin subduction zone at ~50 Ma. However, the Izu-Bonin subduction zone initiated in a roughly E-W orientation further to the south and would not have affected the location or orientation of the subduction zone adjacent South Korea and southern Japan.

Alternative tectonic reconstructions predict the arrival of an E-W oriented mid-ocean ridge to east Asia sometime between 110-80 Ma [*Brown*, 2010; *Engebretson et al.*, 1985; *H. Hara*

and Kurihara, 2010], producing a northward migrating slab window with localized effects in a style similar to that observed along western North America over the last 80 Myr. The uplift of the Sanbagawa Belt and metamorphism of the Ryoke Belt in southwestern Japan during the Late Cretaceous [*Brown*, 2010] and a slightly later metamorphic event due to elevated heat flow, affecting the same Sambagawa Belt at ~75-60 Ma [*H. Hara and Kurihara*, 2010] have both been attributed to localised ridge-trench interaction consistent with this reconstruction. However, these thermal events are not accompanied by a suite of other geological indicators indicative of slab window formation and can be explained by other processes such as the subduction of a seamount or oceanic plateau. Importantly, these tectonic reconstructions use a poorly constrained reconstruction of the Pacific-Kula ridge [*Engebretson et al.*, 1985] as a guide to interpreting geological data in a wider pate tectonic context.

References

Brown, M. (2010), Paired metamorphic belts revisited, *Gondwana Research*, *18*(1), 46-59.

Byrne, T., and L. DiTullio (1992), Evidence for changing plate motions in southwest Japan and reconstructions of the Philippine Sea plate, *Island Arc*, *1*(1), 148-165.

Engebretson, D. C., A. Cox, and R. G. Gordon (1985), Relative motions between oceanic and continental plates in the Pacific Basin, *Spec. Paper Rep. 206*, Geol. Soc. of Am.

Grand, S. P., R. D. van der Hilst, and S. Widiayantoro (1997), Global seismic tomography: A snapshort of convection in the Earth, *GSA Today*, *4*, 1-7.

Hara, H., and K. Kimura (2008), Metamorphic and cooling history of the Shimanto accretionary complex, Kyushu, Southwest Japan: Implications for the timing of out-of-sequence thrusting, *Island Arc*, *17*(4), 546-559.

Hara, H., and T. Kurihara (2010), Tectonic evolution of low-grade metamorphosed rocks of the Cretaceous Shimanto accretionary complex, Central Japan, *Tectonophysics*, *485*(1-4), 52-61.

Lewis, J. C., and T. B. Byrne (2001), Fault kinematics and past plate motions at a convergent plate boundary: Tertiary Shimanto Belt, southwest Japan, *Tectonics*, *20*(4), 548-565.

MacKenzie, J., S. Taguchi, and T. Itaya (1992), Cleavage dating by K-Ar isotopic analysis in the Paleogene Shimanto Belt of eastern Kyushu, SW Japan, paper presented at International geological congress.

Matthews, K. J., R. D. Müller, P. Wessel, and J. M. Whittaker (2011), The tectonic fabric of the ocean basins, *Journal of Geophysical Research*, *116*(B12), B12109.

Montelli, R., G. Nolet, F. Dahlen, G. Masters, E. R. Engdahl, and S.-H. Hung (2004), Finite-frequency tomography reveals a variety of plumes in the mantle, *Science*, *303*(5656), 338-343.

Nakajima, T. (1996), Cretaceous granitoids in SW Japan and their bearing on the crust-forming process in the eastern Eurasian margin, *Geological Society of America Special Papers*, *315*, 183.

Obayashi, M., J. Yoshimitsu, G. Nolet, Y. Fukao, H. Shiobara, H. Sugioka, H. Miyamachi, and Y. Gao (2013), Finite frequency whole mantle P wave tomography: Improvement of subducted slab images, *Geophysical Research Letters*, *40*(21), 5652-5657.
Raimbourg, H., R. Augier, V. Famin, L. Gadenne, G. Palazzin, A. Yamaguchi, and G. Kimura (2014), Long-term evolution of an accretionary prism: The case study of the Shimanto Belt, Kyushu, Japan, *Tectonics*.
Sager, W. W., J. Kim, A. Klaus, M. Nakanishi, and L. M. Khankishieva (1999), Bathymetry of Shatsky Rise, northwest Pacific Ocean: Implications for ocean plateau development at a triple junction, *Journal of Geophysical Research-Solid Earth*, *104*(B4), 7557-7576.
Sagong, H., S. Kwon, and J. Ree (2005), Mesozoic episodic magmatism in South Korea and its tectonic implication, *Tectonics*, *24*(5).
Seton, M., et al. (2012), Global continental and ocean basin reconstructions since 200 Ma, *Earth Science Reviews*, *113*(3-4), 212-270.
Straub, S., S. Goldstein, C. Class, and A. Schmidt (2009), Mid-ocean-ridge basalt of Indian type in the northwest Pacific Ocean basin, *Nature Geoscience*, *2*(4), 286-289.

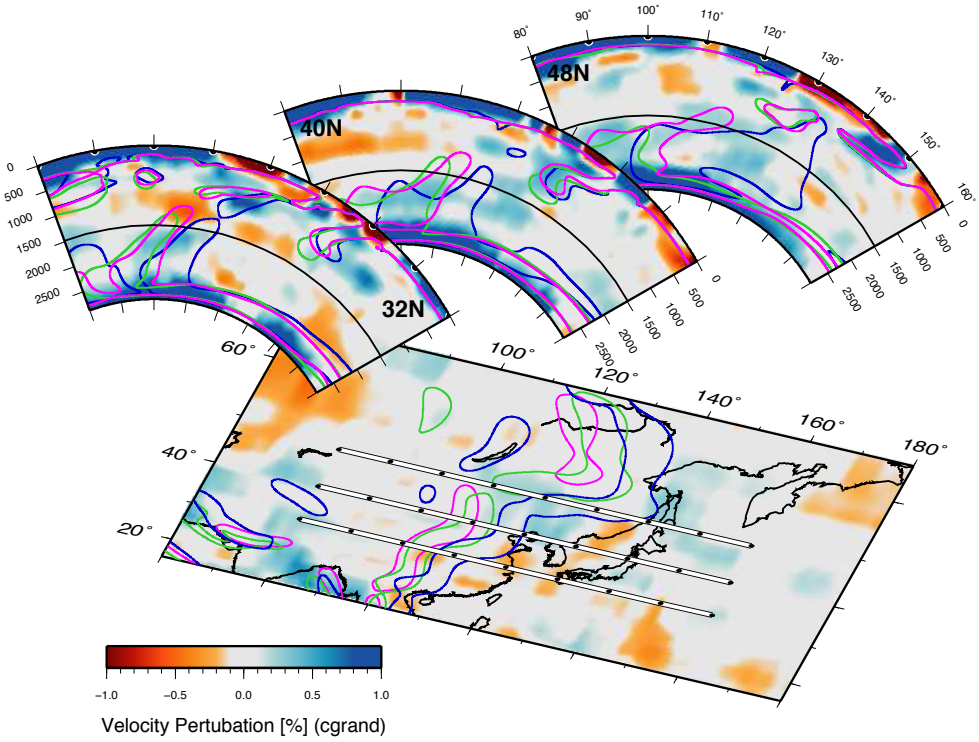

Figure S1.

Perspective view (looking north) of S-wave seismic tomography [*Grand et al.*, 1997] at 1445 km depth and along three vertical cross-sections at 48°N, 40°N and 32°N. Magenta contours correspond to material 10% colder than the ambient mantle from Model 1, green contours from Model 2 and blue contours from Model 3. The horizontal black lines on the vertical cross-sections denote the depth shown in the map.

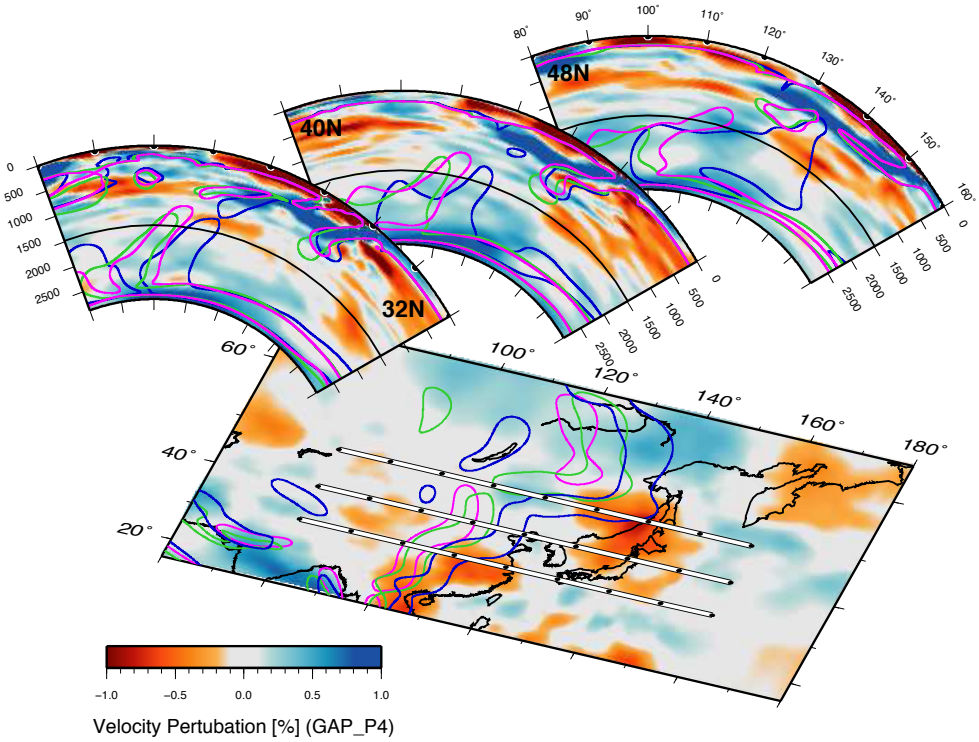

Figure S2.

Perspective view (looking north) of GAP_P4 P-wave seismic tomography [*Obayashi et al.*, 2013] at 1497 km depth and along three vertical cross-sections at 48°N, 40°N and 32°N. Key as for Fig. S1.

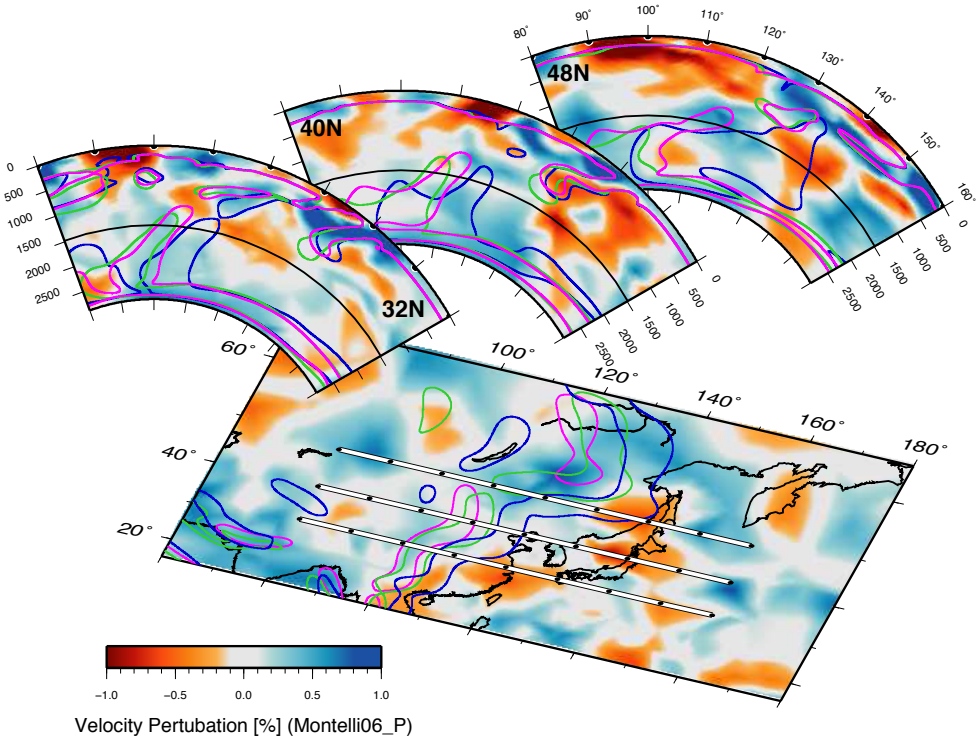

Figure S3.

Perspective view (looking north) of Montelli P-wave seismic tomography [*Montelli et al.*, 2004] at 1500 km depth and along three vertical cross-sections at 48°N, 40°N and 32°N. Key as for Fig. S1.

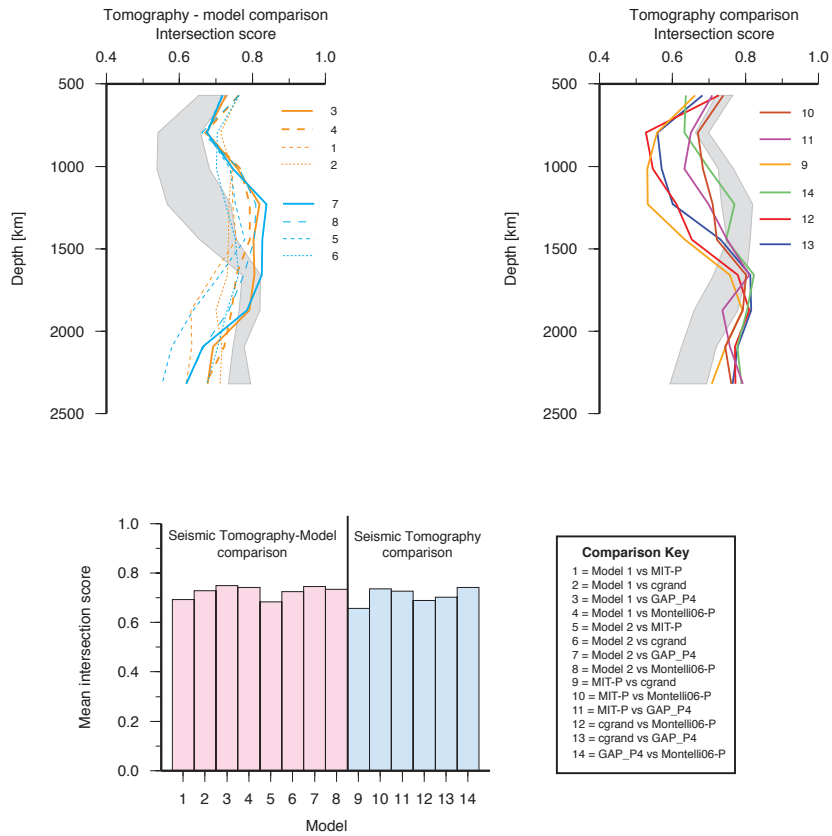

Figure S4.

Intersection scores between seismic tomography and modeled present-day temperature. The top left graph shows the fit or intersection score between the two preferred geodynamic models (Model 1 = orange, Model 2 = blue) and the four seismic tomography models used in this study. The grey envelope shows the mean and standard deviation of the intersection score obtained by comparing seismic tomography models to one another. The top right graph shows the fit between the three P-wave seismic tomography models and the S-wave model. The grey envelope shows the mean and standard deviation of the fit between geodynamic models and seismic tomography models comparison. The bottom histogram shows the mean intersection scores integrated across all depths for each comparison (see key).